American Journal of Engineering and Applied Sciences

Research Article

An Investigation of Mold Cavity Pressure of Self-Clamping Molds During Solid Tire Manufacturing

Sadeep Amantha Mawathage, Jayashingha Arachchige Indika Sanjeewa and Nirosh Dilruk Jayaweera

Department of Mechanical Engineering, University of Moratuwa, Sri Lanka

Article history
Received: 11-02-2025
Revised: 03-04-2025
Accepted: 09-04-2025

Corresponding Author:
Sadeep Amantha Mawathage
Department of Mechanical Engineering, University of Moratuwa, Sri Lanka
Email: mawathagesa.19@uom.lk

Abstract: This study investigates the mold cavity pressure in self-clamping molds used for solid tire manufacturing, a sector where Sri Lanka is a leading global supplier. Our research presents a detailed investigation into the mold cavity pressure of self-clamping molds used in solid tire production. By integrating experimental data, the effects of critical parameters such as clamp bolt torque, final tire temperature, and tire volume on mold cavity pressure were investigated. This knowledge enables engineers to predict and control the pressure distribution during curing, ensuring uniform rubber flow, proper mold filling, and consistent vulcanization. Further, manufacturers can fine-tune clamping force and thermal input to reduce defects such as flash lines, voids, or under-cured regions. It also supports process automation, improves product quality, extends mold life, and minimizes material waste, ultimately enhancing production efficiency and reliability in solid tire manufacturing.

Keywords: Solid Tire, Tire Mold, Plastic Deformation, Cavity Pressure

Introduction

Tires are essential components in vehicles, providing support, traction, and shock absorption. Their structural design and material composition vary significantly depending on application requirements, particularly in terms of load-bearing capacity, surface conditions, and operational durability. Tires are broadly categorized into three main types: pneumatic tires, semi-pneumatic tires, and solid tires. Each type offers distinct advantages and limitations based on its internal construction and the medium used for load transmission.

Pneumatic tires are the most common and widely used type in both passenger and commercial vehicles. These tires are air-filled, featuring an inner tube or a tubeless cavity that holds pressurized air. The air pressure supports the vehicle load and provides the cushioning necessary for a smoother ride over uneven surfaces. Pneumatic tires are characterized by their excellent shock absorption, traction, and fuel efficiency due to lower rolling resistance. However, their susceptibility to punctures and the need for regular inflation maintenance make them less suitable for certain industrial or hazardous environments. According to recent studies (Wong, 2022), pneumatic tires offer optimal dynamic performance but can be vulnerable to heavy-duty and impact conditions.

Semi-pneumatic tires, by contrast, have a structure that mimics pneumatic tires but without air. These tires are often constructed from molded rubber or polymer composites, sometimes featuring internal air pockets or a hollow core that allows limited compression. They offer a compromise between solid and pneumatic tires by retaining some cushioning effects while eliminating the risk of punctures. Semi-pneumatic tires are typically used in low-speed or light-duty applications such as hand trucks, lawnmowers, and some warehouse vehicles. While they provide better durability than pneumatic tires in harsh conditions, they still do not match the shock absorption or energy efficiency of fully pneumatic designs.

The focus of this study: Solid tires, also known as cushion tires, are made entirely from solid rubber or a combination of rubber and polyurethane compounds. These tires contain no air and are highly resistant to punctures, cuts, and wear, making them ideal for industrial applications where vehicles are subjected to heavy loads, sharp debris, or chemically aggressive environments. Solid tires are commonly used in forklifts, airport tugs, and military logistics vehicles, where durability and load capacity outweigh the need for comfort or high-speed mobility. Despite their robustness, solid tires typically exhibit higher rolling resistance and lower shock absorption. Research by Clark (1981) outlines the trade-offs associated with solid tires, particularly in terms of thermal buildup and vibration transmission.

As shown in Figure 1, solid tires are typically composed of multiple layers, each engineered to serve a specific mechanical and functional purpose. The outer

tread layer is made of highly wear-resistant rubber and is responsible for providing traction, absorbing surface irregularities, and resisting abrasion during operation. Beneath the tread, the middle cushion layer acts as a shock-absorbing buffer that dissipates stresses and enhances ride comfort by reducing vibrations and impacts transferred from the ground. At the core lies the base or core layer, which is usually reinforced with hard rubber or embedded steel rings. This layer provides a secure attachment to the rim, maintains structural integrity under heavy loads, and transmits torque between the tire and the wheel hub. Some solid tires may also include sidewall stiffeners or grooves to facilitate heat dissipation and improve lateral stability. Together, these components enable the solid tire to provide excellent durability, load-bearing capacity, and puncture resistance, making them ideal for industrial, construction, and material handling applications.

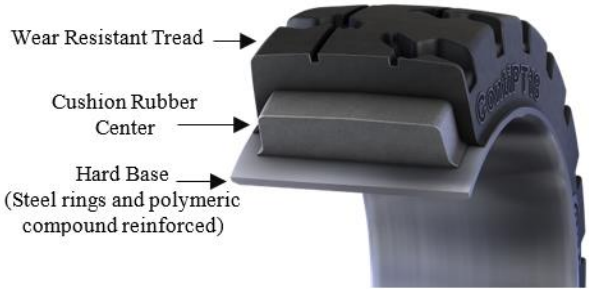

Fig. 1: Components of a Solid Tire

The manufacturing of solid tires involves a sequence of operations as illustrated in Figure 2, including material preparation, molding, and curing, tailored to produce tires with high load-bearing capacity and durability. The process begins with the mixing of natural and synthetic rubber compounds, reinforced with fillers such as carbon black and silica to enhance strength and wear resistance. These compounds are shaped into green tires and placed into precision-machined molds. The molding is typically done using compression or transfer molding techniques due to the solid structure of the tire. Once inside the mold, the rubber is subjected to high pressure and heat, initiating the vulcanization (curing) process, which chemically cross-links the polymer chains, imparting elasticity and mechanical integrity. The mold is then opened, and the tire is cooled, trimmed, and inspected for dimensional accuracy and defects (Shanbag & Manjare, 2020). Sri Lanka stands out as a prominent manufacturer of industrial solid tires, commanding a market share of approximately 20-25%, with solid tires constituting 61% of the export value of the rubber products of Sri Lanka (Bragov *et al.*, 2019; Vidyaratne, 2022). These tires are crucial for ensuring the stability and safety of heavy-duty vehicles, thereby implying the importance of reliable production processes.

Among these manufacturing stages, molding process is critical to achieve consistent output quality and performance of t. There are several molding techniques used in tire manufacturing, primarily determined by the tire type, production volume, and required performance. Compression molding is widely used for solid and industrial tires due to its simplicity and cost-effectiveness, though it suffers from longer cycle times and lower dimensional accuracy (Dasgupta, 1993). Transfer molding improves compression by allowing better control of material flow and is suited for intricate designs, but it requires more complex tooling and performed rubber charges. Injection molding offers high-speed, automated production with excellent precision, making it ideal for small solid tires, though it demands expensive equipment and is less suitable for large tires (Clark, 1981). Finally, steam dome or segment molding is predominantly used in pneumatic tire manufacturing, offering uniform heat and pressure distribution for complex radial designs, but its high setup complexity and sensitivity to alignment make it resource intensive. Each method balances trade-offs between cost, precision, and scalability, guiding its suitability for specific tire applications.

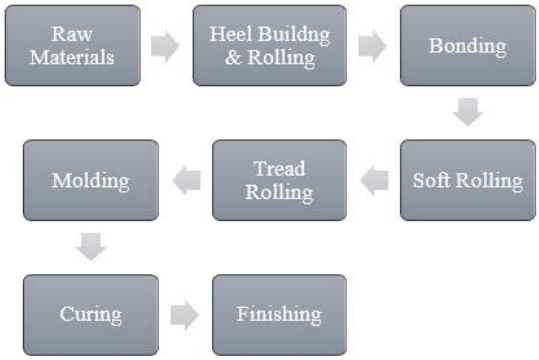

Fig. 2: Solid Tire Manufacturing Process

Tire molds that are utilized in compression molding can be classified into two categories: "Casing Type - Self Clamping Mold" and "Press Type - Press Clamping Mold," based on their structural design and the curing process employed (Smith, 1970). In this study, Casing Type - Self Clamping Mold is considered due to local availability on data acquisition, as illustrated in Figure 3-a, with labelled mold parts and their separation surfaces.

From a manufacturing perspective, the precision of the mold directly affects the final shape, size, and tread pattern of the tire. This includes the alignment of the upper and lower mold halves, cavity profile, and venting systems. If the mold components do not fit together within tight tolerances, flash lines (excess material seams), asymmetry, and voids may occur in the final product, impacting both aesthetics and functionality. The requirement becomes even more stringent in self-clamping molds, where the internal locking mechanism relies on exact alignment for effective sealing and pressure containment. This is because the vulcanization occurs at 140-200°C in the mold and the curing duration can vary, taking between 30 to 60 minutes depending on

the size and composition of the materials (Kern *et al.*, 2004). During this process, a considerable buildup of internal pressure is generated in the mold cavity due to the incompressible volumetric expansion of the rubber material.

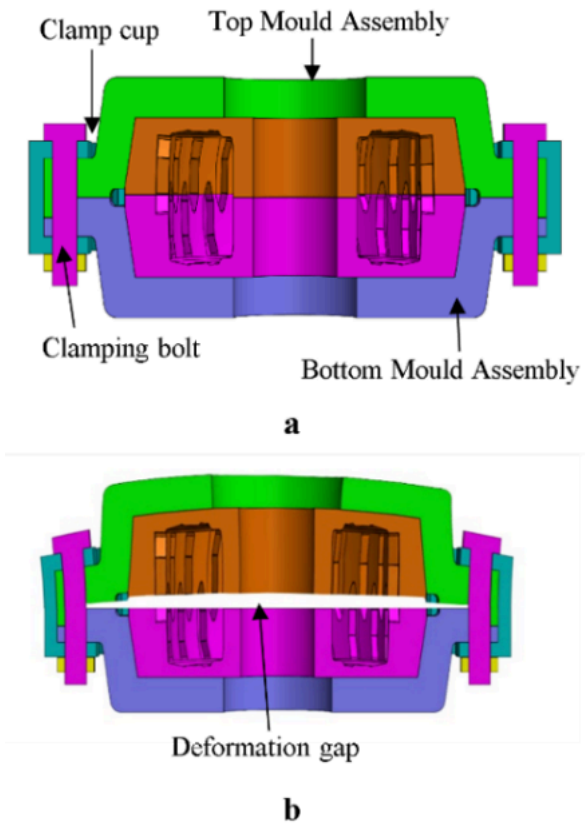

Fig. 3: a) Mold components, b) Deformed Mold

Fig. 4: Mold surface change over (Left: Before, Right: After) several vulcanizations

Carbon alloy steels are frequently used as the material of the mold parts, susceptible to deformation and cracks which affect dimensional quality and safety. Furthermore, the repetitive cycles inherent in tire molding present significant challenges, including the potential failure of mold components due to plastic deformation and crack propagation as illustrated in Figure 4. Such failures not only compromise the dimensional tolerances of the tires but also jeopardize overall safety standards. Therefore, a comprehensive understanding of these issues and the implementation of effective mitigation strategies are essential for maintaining consistent and secure production processes (Dasgupta, 1993). Any deformation in the mold compromises its ability to produce tires with the requisite shape and dimensions. Consequently, designers of tire molds must prioritize the development of mold components that possess high-strength capabilities, enabling them to withstand various loads and boundary conditions (Manson, 1965), preserving the longevity of part life.

Several critical factors contribute to failures in tire mold parts, including design flaws, manufacturing imperfections, and material fatigue. Although researchers have begun to investigate the behavior of strain hardening and the sensitivity of materials to strain rate (Smith, 1970), further investigations are required to clarify the temperature-dependent plastic deformation of materials and to develop comprehensive models that can accurately predict deformation under varying temperature conditions (Fragassa & Ippoliti, 2016; Lekarp & Dawson, 1998). Additionally, research should concentrate on understanding plastic deformation during different forming processes and examining the effects of microstructural changes on deformation behavior. Hence, current studies do not adequately examine the relationship between these factors and mold cavity pressure calculations. This hinders optimal tire mold design and the resolution of pressure-related failures in components, which are shown in Figure 5. Addressing these gaps is essential for advancing both theoretical understanding and optimization of practical applications within the field of tire manufacturing.

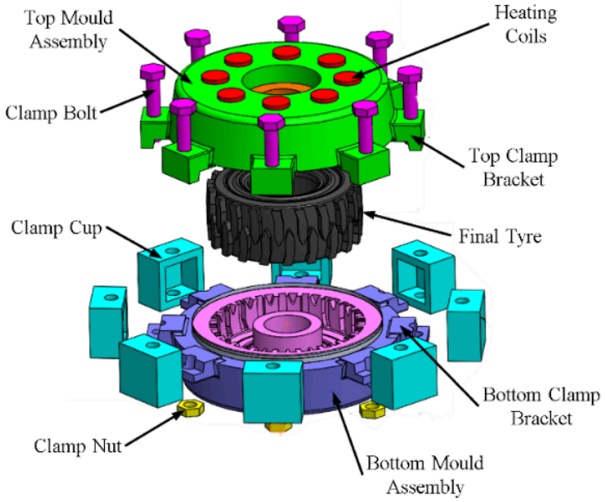

Fig. 5: Tire with a molding assembly

Considering the current knowledge, the true stress-strain curve is called a flow curve because it provides the pressure (σ) for a substance to provide a wide range of materials under certain conditions. Other important factors affecting pressure and strain curve are grid/strain ratio (ε), and temperature of the object (Eskandari & Kim, 2014). Equation (1) as defined by Lee *et al.* (2009)

is considered the most common equation which defines the material flow behavior:

$$\sigma = K\varepsilon^{n} \quad (1)$$

Where K and n are the strength coefficient and strain-hardening exponent. The strain-hardening exponent n ranges from 0 to 1, where n = 0 represents a perfectly plastic solid, and n = 1 corresponds to an elastic solid. For most common metals, the values of n typically range between 0.10 and 0.50. The above equation, known as the Power law equation, is also referred to as the Holloman-Ludwig equation (Kern *et al.*, 2004).

In this study, an experimental setup was designed to measure pressure values under three distinct parameters: clamp bolt torque, final tire temperature, and tire volume. The data obtained were analyzed to identify the behavior of cavity pressure with respect to the changes of selected variables.

Materials and Methods

This section outlines the comprehensive research methodology and the specific focus of this paper, which is deriving trendlines for the mold cavity pressure calculation. To facilitate this analysis, meticulous experimental procedures and numerical simulations are employed. The flow chart in Figure 6 provides a clear and concise overview of the research procedures, which are essential for understanding the results and conclusions of the study. The investigation focuses on two principal aspects: plastic deformation during the tire curing process and fatigue life calculations for mold components.

Fig. 6: Research Methodology

Parameters and Design Variables Selection

As the pressure of the mold cavity results in the plastic deformation of the mold, the parameters which influence the permanent deformation of metals: temperature, pressure load, clamp bolt torque were selected to be considered as the variables of the experimental procedure (Bragov *et al.*, 2019). Furthermore, during the tire curing operation, heat energy is provided to the raw tire to give its final shape. The rubber volume inside the mold cavity expands due to this heat energy, as a result, it builds up pressure and increases the mold gap opening as demonstrated in Figure 7 (Zhuang & Cheng, 2011).

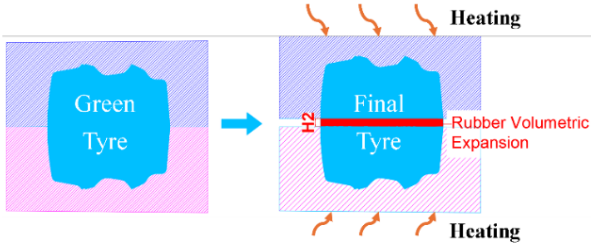

Fig. 7: Thermal expansion of the tire inside the mold

- ΔV: Rubber volume expansion due to heat
- β: Rubber Volumetric expansion coefficient
- V_0: Initial Raw Tire Volume
- ΔT: Temperature difference between final & raw tire
- H_1: Expected mold opening without clamping
- H_2: Measured Mold opening due
- ε: Tire Compressive Strain

The equation for the change in volume is given as follows (Pluta and Hryniewicz, 2012):

$$\Delta V = \beta \cdot V_0 \cdot \Delta T \quad (2)$$

$$\Delta V = H_1 \cdot A \quad (3)$$

From (2) and (3)

$$H1 = \beta \cdot V_0 \cdot \Delta T / A \quad (4)$$

$$\varepsilon = (H_1 - H_2) / H_1 \quad (5)$$

Therefore, tire volume (mold cavity volume) was identified as a crucial parameter of the pressure created within the mold. Hence, the experiment procedure was developed to have three variables: clamp bolt torque, final tire temperature and tire (mold cavity volume). It was decided to obtain a dataset by varying one parameter at a time to clearly observe the effect of the respective parameter.

Experimental Setup

The setup includes a solid tire mold which replicates the manufacturing conditions (Figure 8), a piezoelectric melt pressure sensor (4021B05H2P1 pressure transducer) in contact with the mold, and other regulating

DOI: 10.3844/ajeassp.2025.89.97

devices to adjust the pressure within the cavity during the test (Figure 9).

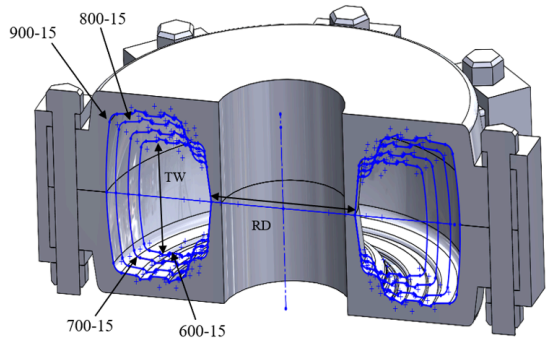

Fig. 8: Cross section of the tested molds (Notation Tire Width × 100 – Rim Diameter in inches)

Fig. 9: Experimental Setup

The data are obtained and stored using a data acquisition system. The piezoelectric melt pressure sensor was installed with the following control system, which is attached to the mold cavity, as per the below-described transducer installing guideline. This pressure sensor system consists of a consignor head, detector circuit, signal amplifier unit, 24V power supply, STG analogue to digital converter, and PC with DEWE software interface as illustrated in Figure 10. The sensor is calibrated to zero at the atmospheric pressure and ambient temperature in the factory, in the built-in state with the application of the correct torque value (Zhuang & Cheng, 2011). The procedure employed the following assumptions for the convenience of the study while preserving accuracy.

- The properties of the tire rubber compound, including compression modulus, compression strength, elongation, and viscosity, remained constant throughout the tire molding process.
- The rubber compound material retained its solid state and did not undergo any phase changes during the tire curing cycle.
- The tire rubber material is uniform and consistent throughout the entire volume of the tire.
- The pressure and temperature gradients are consistent and evenly distributed during the tire curing process.

The sensor was fixed and inserted into the prepared M8x1:25 threaded hole and 40 Nm torque was applied (Figure 11). The mold was inserted and mounted to the curing press. The pressure testing experimental setup with the measuring equipment and accessories was prepared and the computer was turned on. Then the press was operated to open the mold (Figure 12), and the 4790ASP2-2m extension cable was connected to the sensor and the AC/DC power supply (200W, 24V). The curing cycle was started by activating the heating elements connected to the mold, and the "DEWESoft" application was opened.

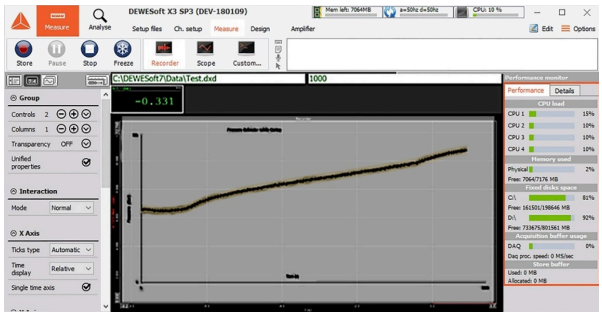

Fig. 10: DEWEsoft User Interface during pressure data recording

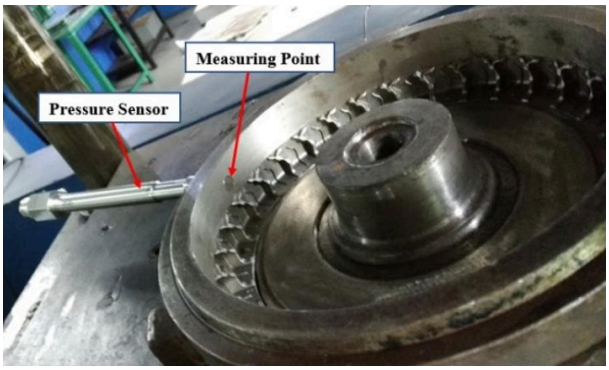

Fig. 11: Pressure Measurement Point

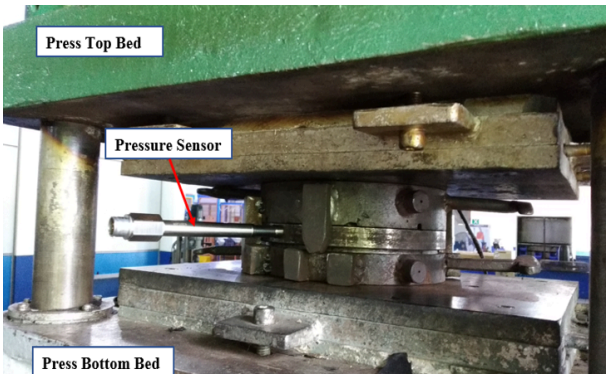

Fig. 12: Pressure measuring system

Pressure Testing Procedure

It was utilized for pressure sensor signal processing and storing the pressure versus time within the historical data logger. Eight drill holes at equal intervals were placed in the circumference of the mold, where the pressure transducers were fixed for separate experiments,

ensuring the other seven holes were properly sealed with lids. The pressure values and pressure versus time graphs were recorded. Four pressure measurement experiments were conducted for each tire to calculate the average maximum pressure and standard deviation (Olabanji *et al.*, 2020).

Results

To observe the behavior of the cavity pressure with respect to changes of each variable, the following three cases were tested.

- Case 1: Clamp Bolt Torque Variation (Final Temperature: 140 °C, Volume: 0.01 m^3)
- Case 2: Final Temperature Variation (Bolt Torque: 200 Nm, Tire Volume: 0.01 m^3)
- Case 3: Tire (Cavity) Size Variation (Final Temperature: 120 °C, 170 Nm)

The obtained results were graphed and generated both linear and quadratic equations to model the variation as follows.

Case 1: Clamp Bolt Torque Variation

The first experiment was conducted with this sample tire mold, maintaining identical temperature increment across all scenarios to examine the pressure behavior within the mold cavity. This was specifically focused on the relationship between the pressure and the gap between the top and bottom mold assemblies after securing the clamp units. During this process, it was essential to record the requisite bolt torque corresponding to the measured mold opening gap. This methodical approach allows for a detailed analysis of how variations in bolt torque influence the pressure dynamics within the mold cavity, thereby providing insights into optimizing mold design parameters for enhanced performance and durability.

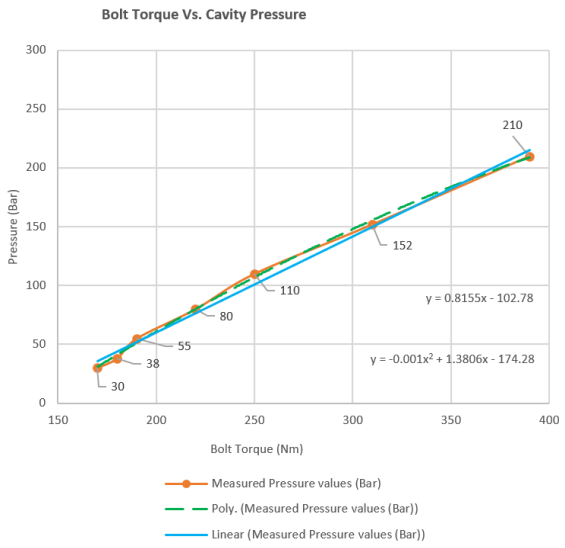

Fig. 13: Bolt Torque vs. Cavity Pressure Results

Case 2: Final Temperature Variation

The second experiment was performed using the same above-mentioned sample tire mold by maintaining the constant bolt torque for all scenarios to investigate the mold cavity pressure concerning the gap between the top and bottom mold assemblies after fixing the clamp units. Final tire temperature and the maximum mold opening gap were recorded through the procedure. The mold gap (H) was measured by changing the final tire temperature.

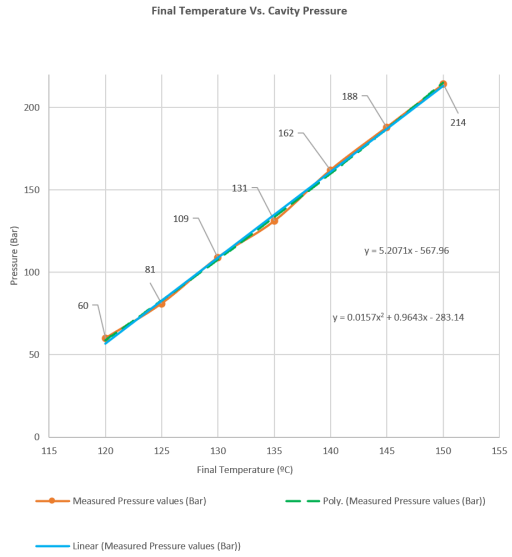

Fig. 14: Final Temperature vs. Cavity Pressure Results

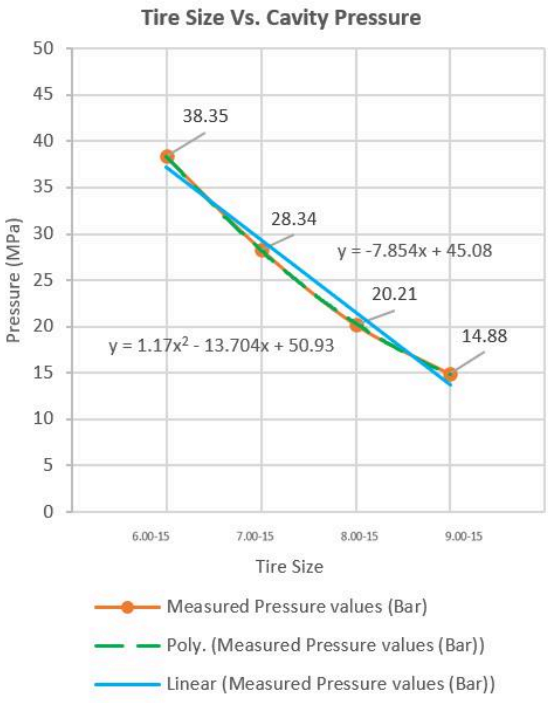

Fig. 15: Tire Size vs. Cavity Pressure Results

Case 3: Tire (Cavity) Size Variation

The third experiment was performed using the four different sizes of tire molds by maintaining the constant bolt torques and final tire temperatures. The mold gap (*H*) was measured by changing the tire volume. The measured mold internal pressure values were decreased when the tire volume increased.

Discussion

The pressure builds up inside the mold cavity evidently depends on the below three parameters, which enables the pressure to be written as a function of these parameters.

1. (ΔT) – Temperature increment from raw tire temperature to final tire.
2. (H) – Mold opening gap between the top and bottom mold assemblies due to the thermal expansion of the tire.
3. (V) – Initial raw tire/mold cavity volume.

The solid tire mold cavity pressure, P = f [ΔT, H, V]

According to the experimental data we obtained, the following insights and trendlines could be identified.

Case 1: Clamp Bolt Torque Variation

The test results (Figure 13) examining the relationship between bolt torque and cavity pressure in a solid tire mold reveal critical insights into the interplay of mechanical tightening forces and internal pressure dynamics. The linear regression model ($y = 0.8155x - 102.78$) suggests a direct proportionality between bolt torque and cavity pressure, indicating that increasing torque generally elevates pressure within the mold. However, the quadratic model ($y = -0.001x^2 + 1.3806x - 174.28$) introduces a non-linear component, highlighting that the pressure increase diminishes at higher torque levels. This curvature, governed by the negative coefficient of the x^2 term, implies potential saturation effects or material resistance limiting further pressure gains beyond a specific torque threshold.

Case 2: Final Temperature Variation

The analysis of final temperature versus cavity pressure (Figure 14) in a solid tire mold, under a fixed bolt torque of 200 Nm and tire volume of 0.01 m³, demonstrates a significant dependence of internal pressure on thermal conditions. The linear regression model ($y = 5.2071x - 567.96$) indicates a strong positive correlation, with each unit increase in temperature contributing approximately 5.2 Bar of pressure. However, the large negative intercept suggests this model may not be physically meaningful at lower temperatures, as it predicts unrealistic negative pressures. This implies the linear relationship is likely valid only within the tested temperature range (e.g., 115–155 units, assumed to be °C). The quadratic model ($y = 0.0157x2 + 0.9643x - 283.14$), with its positive x^2 coefficient, reveals an accelerating pressure increase at higher temperatures. This non-linearity suggests that thermal expansion or material softening effects dominate as temperatures rise, amplifying pressure gains beyond what a linear model predicts. For instance, at 150°C, the quadratic model predicts a pressure increase of ~20 Bar per 10°C temperature rise, compared to the linear model's ~52 Bar per 10°C. Such behavior underscores the importance of temperature control in high-heat conditions to avoid over-pressurization risks, such as mold deformation or material degradation.

Case 3: Tire (Cavity) Size Variation

The small tires build higher internal mold pressure values and the larger tires build lower pressure (Figure 15). The quadratic equation ($y = 1.17x^2 - 13.704x + 50.93$) indicates a non-linear trend where pressure initially decreases with increasing tire size, reaching a minimum before rising again at larger volumes. This U-shaped behavior suggests competing mechanisms: at smaller tire sizes, geometric constraints or material compression may dominate, reducing pressure, while at larger sizes, thermal expansion or volumetric strain under fixed torque could drive pressure upward. In contrast, the linear model ($y = 7.854x + 45.08$) implies a steady pressure increase with tire size, potentially oversimplifying the system's dynamics.

The measured pressure values (28.34, 20.21, and 14.88 MPa) align more closely with the quadratic model's initial downward trend, as they decrease with increasing tire size. For example, at smaller volumes, higher pressures (e.g., 28.34 MPa) may result from concentrated forces in confined spaces, while intermediate sizes (20.21 MPa) reflect reduced constraints. However, the quadratic model predicts a reversal in this trend at larger sizes, which is not captured in the provided data. This highlights the need for additional measurements to validate the model's extrapolation beyond the tested range.

Conclusion

The investigation into cavity pressure dynamics within solid tire molds, considering the variables bolt torque, temperature, and tire size, highlights multifactorial dependencies critical to manufacturing optimization. Key findings reveal:

1. Bolt Torque: A quadratic relationship governs pressure at higher torque levels, with diminishing returns beyond optimal thresholds, emphasizing the need to balance mechanical input with material constraints.
2. Temperature: Pressure exhibits accelerating non-linear growth at elevated temperatures, necessitating stringent thermal control to mitigate over-pressurization risks.

3. Tire Size: A U-shaped quadratic trend suggests pressure minima at intermediate sizes, underscoring the importance of geometric and volumetric considerations in process design.

While linear models provide simplicity for narrow operational ranges, quadratic approximations better capture system complexity, particularly under extreme conditions. Practical applications must prioritize model-informed parameter calibration to ensure uniform pressure distribution, energy efficiency, and equipment longevity. Limitations, such as restricted data ranges and unvalidated extrapolations, call for expanded experimental validation and integration of statistical metrics to refine predictive accuracy.

From an energy standpoint, understanding the relationship between cavity pressure, bolt torque, tire volume, and temperature allows manufacturers to reduce cycle times and eliminate overcuring, thereby minimizing unnecessary energy consumption during the heating and pressurization stages of curing. In terms of the environment, this study supports cleaner manufacturing by reducing rubber waste and defective output through better process control and material flow prediction. Consistent curing and pressure distribution lead to higher-quality products with fewer rejections, lowering the need for rework and the associated material, water, and energy waste. Moreover, enhanced durability of the solid tires, because of better mold design, extends their service life, reducing the frequency of replacements and the environmental burden associated with rubber processing and disposal. Finally, from an economic perspective, this research drives cost reduction by streamlining the production process.

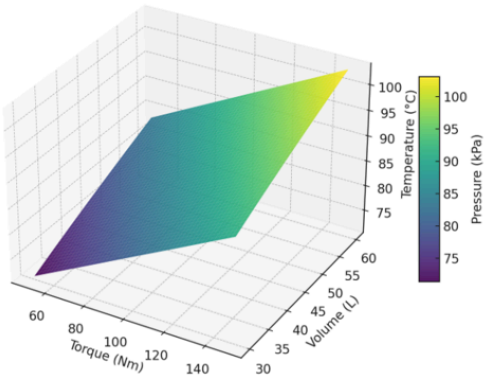

Fig. 16: 3D Pressure Distribution

Future Work

The experimental investigations into cavity pressure dynamics; spanning bolt torque, temperature, and tire size have yielded critical insights that directly inform the next phase of research. The observed non-linear relationships highlight the necessity of a multivariate predictive model to adequately capture interdependencies between these variables. Building on the empirical foundation established here, the following steps are proposed:

Development of a 3D Surface Model

By expanding the data collection, a 3D surface graph (Figure 16) will map pressure as a function of temperature, bolt torque, and cavity volume. This model will integrate the quadratic and linear relationships identified in earlier tests, enabling predictive accuracy across broader operational ranges. For instance, the U-shaped pressure trend with tire size and the torque-dependent saturation effects will be foundational to this multidimensional analysis.

Predictive Function for Design Optimization

Advanced curve-fitting methodologies will generate a unified mathematical function from the 3D dataset. This function will empower engineers to predict cavity pressure under any combination of the tested parameters, streamlining the design of new tire molds. Notably, the experimentally validated trends (e.g., pressure minima at intermediate tire sizes, optimal torque thresholds) will ensure the model's relevance to real-world scenarios.

Validation Framework for New Mold Designs

Prior to production, pressure predictions for novel mold designs will be cross-verified against experimental data from comparable tire sizes (as demonstrated in Figures 8–10). This iterative validation process, grounded in the robust empirical results of this study, will minimize trial-and-error prototyping, reduce costs, and enhance mold durability.

Further, the current experiments have already resolved key uncertainties:

- Identified optimal torque ranges (e.g., diminishing returns beyond 110 Nm) to avoid over-pressurization.
- Quantified temperature sensitivity (e.g., ~5.2 Bar/°C linear rise, accelerating non-linearity at high temperatures).
- Revealed tire size-dependent pressure minima, critical for balancing geometric constraints and material behavior.

These outcomes not only validate the necessity of multifactorial analysis but also provide a scalable framework for future industrial applications. By bridging empirical data with predictive analytics, this work lays the groundwork for smarter, data-driven mold design that ultimately advancing manufacturing efficiency, product consistency, and equipment longevity.

Acknowledgment

The authors are grateful to all institutions and individuals who contributed to this study.

Funding Information

The authors declare no financial support or funding for this study.

Author's Contributions

Sadeep Amantha Mawathage: Designed the study framework and contributed to writing and revising the manuscript.

Jayashingha Arachchige Indika Sanjeewa: Conceptualized the research idea, provided technical expertise in developing the manuscript and conducted the experimental procedure.

Nirosh Dilruk Jayaweera: Reviewed and provided critical feedback on the manuscript.

Ethics

This article is original and contains unpublished material. The corresponding author confirms that all the other authors have read and approved of the manuscript, and the study follows ethical guidelines and contains no conflicts of interest or harm to humans, animals, or the environment.

References

Bragov, A., Igumnov, L., Konstantinov, A., Lomunov, A., & Rusin, E. (2019). Effects of High Strain Rate and Self-heating on Plastic Deformation of Metal Materials Under Fast Compression Loading. *Journal of Dynamic Behavior of Materials*, *5*(3), 309–319. https://doi.org/10.1007/s40870-019-00214-x

Clark, S. K. (1981). *Mechanics of pneumatic tires*.

Dasgupta, A. (1993). Failure mechanism models for cyclic fatigue. *IEEE Transactions on Reliability*, *42*(4), 548–555. https://doi.org/10.1109/24.273577

Eskandari, H., & Kim, H. S. (2014). A Theory for Mathematical Framework of Fatigue Damage on S-N Plane. *Key Engineering Materials*, *627*, 117–120. https://doi.org/10.4028/www.scientific.net/kem.627.117

Fragassa, C., & Ippoliti, M. (2016). *Technology Assessment of Tire Mould Cleaning Systems and Quality Finishing*.

Kern, T.-U., Abe, F., & Viswanathan, R. (2004). *Creep-resistant steels*.

Lee, J., Lee, C., & Kim, B. (2009). Reverse analysis of nano-indentation using different representative strains and residual indentation profiles. *Materials & Design*, *30*(9), 3395–3404. https://doi.org/10.1016/j.matdes.2009.03.030

Lekarp, F., & Dawson, A. (1998). Modelling permanent deformation behaviour of unbound granular materials. *Construction and Building Materials*, *12*(1), 9–18. https://doi.org/10.1016/s0950-0618(97)00078-0

Manson, S. S. (1965). Fatigue: A complex subject—Some simple approximations. *Experimental Mechanics*, *5*(4), 193–226. https://doi.org/10.1007/BF02321056

Olabanji, O., Mpofu, K., & Battaia, O. (2020). A distributive approach for position control of clamps in a reconfigurable assembly fixture. *International Journal of Automation and Control*, *14*(1), 34. https://doi.org/10.1504/ijaac.2020.103804

Pluta, Z., & Hryniewicz, T. (2012). Thermal Expansion of Solids. *Journal of Modern Physics*, *03*(08), 793–802. https://doi.org/10.4236/jmp.2012.38104

Shanbag, A., & Manjare, S. (2020). Life Cycle Assessment of Tyre Manufacturing Process. *Journal of Sustainable Development of Energy, Water and Environment Systems*, *8*(1), 22–34. https://doi.org/10.13044/j.sdewes.d7.0260

Smith, K. N. (1970). *A Stress-Strain Function for the Fatigue of Metals*.

Vidyaratne, K. A. C. (2022). Review on National Competitive Advantage for Marketing Potentials for Off-The Road (OTR) Tyre Industry in Sri Lanka. *Sri Lanka Journal of Marketing*, *8*(2), 150–164. https://doi.org/10.4038/sljmuok.v8i2.105

Wong, J. Y. (2022). *Theory of Ground Vehicles*. https://doi.org/10.1002/9781119719984

Zhuang, Z., & Cheng, B. (2011). A novel enriched CB shell element method for simulating arbitrary crack growth in pipes. *Science China Physics, Mechanics and Astronomy*, *54*(8), 1520–1531. https://doi.org/10.1007/s11433-011-4385-y